Bulgarian Chemical Communications, Volume 48, Special Issue E (pp. 297 - 305) 2016

Effect of reservoir on controllable loop thermosyphon

Jingyu Cao[1], Gang Pei[*,1], Yuehong Su[2], Anjum Munir[3], Jing li[*,1], Wang Yunyun[4]

[1] *Department of Thermal Science and Energy Engineering, University of Science and Technology of China, Hefei 230027, China*

[2] *Departments of Architecture and Built Environment, Engineering, University of Nottingham, Nottingham*

[3] *Department of Energy Systems Engineering, University of Agriculture, Faisalabad-Pakistan*

[4] *Key Laboratory of Optoelectronic Devices and Systems of Ministry of Education and Guangdong Province, College of Optoelectronic Engineering, Shenzhen University, Shenzhen 518060, China*

The controllable loop thermosyphon (CLT) has the potential to be utilized in various applications, including cool-storage refrigerators powered by solar energy and electricity with the time-of-use price policy. An active control method can be achieved by interrupting the two-phase natural circulation flow of CLTs. However, the precise temperature control performance of CLTs under active control depends on the system design and should be optimized. In this study, CLTs with and without a reservoir were designed and tested. Valves were added to the vapor and liquid lines. Therefore, three control modes were available to start and stop the heat transfer process of the CLTs. A series of experiments was conducted to compare the start–stop and heat transfer performances of the two CLTs at various R134a fill ratios and heat sink temperatures. The heat transfer performance of the CLT with a reservoir was more stable than that of the CLT without a reservoir. The reservoir degraded the start–stop performance of CLT in control mode A. The start–stop performances of the two CLTs were similar in control mode C. The CLTs in control mode C started up in approximately 20–25 s and stopped in about 70–80 s. Results revealed that an optimal system design could be selected under different application backgrounds.

Keywords: refrigerator, loop thermosyphon, reservoir, start–stop performance

INTRODUCTION

Phase-change materials (PCMs) are widely used in refrigerators to save energy, reduce cost, and protect the environment. Cool-storage refrigerators present significant advantages and promising prospects.

The solar photovoltaic (PV) vapor compression refrigerator is the most common solar-powered refrigerator [1–3]. In traditional PV refrigerators, storage batteries are adopted widely because of the unstable solar energy. High-priced batteries cause considerable energy wastage in the charge–discharge process [4]. Siaka Toure and Foster et al. designed and investigated battery-free cool-storage refrigerators. Their results showed that the cooling capacity of ice is completely adequate for a few days of operation without a power input [5, 6]. PV cool-storage refrigerators provide significant advantages in terms of cost and efficiency; however, they cannot control the temperature of fresh food precisely when their compressors stop working. This disadvantage is caused by the low heat transfer rate between PCM and the air in fresh food compartments.

Cool-storage refrigerators are more efficient than traditional direct-cooling refrigerators [7–10]. Moreover, the time-of-use price policy has been implemented worldwide because of the significant difference between peak and valley power demands [11]. Cool-storage refrigerators are a major energy-consuming home appliance and demonstrate the potential to stabilize electric grids and reduce electricity costs [12]. However, similar to PV cool-storage refrigerators, they have the disadvantage of imprecise temperature control.

The fresh food compartment temperatures of cool-storage refrigerators are controlled by the start–stop mechanism of compressors when powered by electricity. This temperature control mechanism is similar to that of traditional direct-cooling refrigerators without frequency conversion functions [13–15]. The start–stop frequency increase of a compressor can decrease the coefficient of performance of refrigeration systems directly. Thus, the temperature control performance of traditional and cool-storage refrigerators is difficult to improve.

A novel cool-storage refrigerator was proposed in this study to overcome these shortcomings. A loop thermosyphon, which is also referred to two-phase thermosyphon loop, was employed to control the temperature of fresh food. Fig.1 shows that the fresh food compartment is located at the bottom of the refrigerator, and the evaporator is located in the freezer only. The compressor in this novel cool-storage refrigerator can operate continuously for half a day to cool the freezer and store cold energy.

* To whom all correspondence should be sent:
peigang@ustc.edu.cn; lijing83@ustc.edu.cn

The temperature of the fresh food compartment is controlled only by the intermittent heat transfer of the loop thermosyphon. With the long-running compressor and frequent start–stop loop thermosyphon, the efficiency of the refrigeration system and the precision of temperature control improved significantly. Active control of the loop thermosyphon in this novel cool-storage refrigerator was achieved by artificially interrupting its two-phase natural circulation flow. The performance of the precise temperature control of the loop thermosyphon under active control is highly important and requires further investigation.

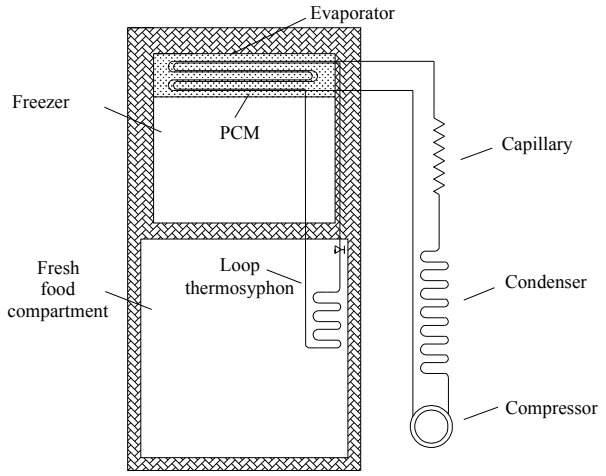

Fig.1. Simplified sample configuration of the novel cool-storage refrigerator

Various characteristics of the loop thermosyphon have been studied since the 1980s [16]. Rahmatollah Khodabandeh and Richard Furberg analyzed the two-phase flow instabilities of a loop thermosyphon with R134a as a refrigerant and found that copper nano- and micro-porous structures decrease the oscillations and enhance the heat transfer coefficient [17]. Yu Song et al. focused on nucleate boiling heat transfer in a helium loop thermosyphon coupled with a cryocooler. The error of the proposed correlation was within 30% in the regime of two-phase nucleate boiling [18]. Jiang He et al. investigated the effect of non-condensable gas on the startup of a loop thermosyphon. No failed startups occurred during any of the tests [19]. Chehade et al. investigated the performance of a loop thermosyphon with water as a working fluid. Their results showed that the optimal fill ratio is between 7% and 10% [20]. Ali Chehade et al. performed experimental and simulative research on a loop thermosyphon for cooling with zero electrical consumption. A new model was proposed and confirmed by experimental data [21]. Ji Li et al. investigated the performance of an insert-type loop thermosyphon for split-type solar water heaters. The experimental system displayed an improvement of 100% in water heating speed [22]. Penglei Zhang et al. studied the performance of a loop thermosyphon with a partially liquid-filled downcomer. A visual test bench was established, and a partially liquid-filled phenomenon was discovered in the downcomer [23]. Zhen Tong et al. investigated an R744 loop thermosyphon used to cool a data center. The R744 loop thermosyphon functioned under a small driving temperature difference of 5 °C, and a theoretical model was utilized to calculate thermal resistance [24]. These experimental and theoretical studies revealed the attractive and comprehensive performance of loop thermosyphons. Thus, loop thermosyphons have been utilized widely in solar applications, electronic equipment cooling, air conditioning, nuclear reactors, waste heat recovery, and other heat transfer fields [25]. However, precise temperature control ability under active control has been neglected. A cool-storage refrigerator combined with a loop thermosyphon remains an unexplored but attractive field.

The performance of the precise temperature control of a controllable loop thermosyphon (CLT) under active control depends largely on the system design. The effect of a reservoir on the precise temperature control performance of CLT within a known range has not been reported. In our previous study, we evaluated the performance of a CLT without a reservoir [26]. On this basis, we designed and tested CLTs with and without a reservoir in the current study. Two valves for each CLT were added to the vapor and liquid lines. Therefore, three control modes were available to start and stop the heat transfer process of the CLTs. A series of experiments was conducted to compare the start–stop and heat transfer performances of the two CLTs at various R134a fill ratios and test conditions.

EXPERIMENTAL SETUP

Operating principle of CLT

The two-phase natural circulation flow in a CLT is presented in Fig.2. The liquid working fluid evaporates in the evaporator and flows to the condenser through the vapor line. The vapor working fluid condenses to the liquid phase in the condenser and flows back through the liquid line to

the evaporator again. The working fluid flows automatically with the assistance of gravity.

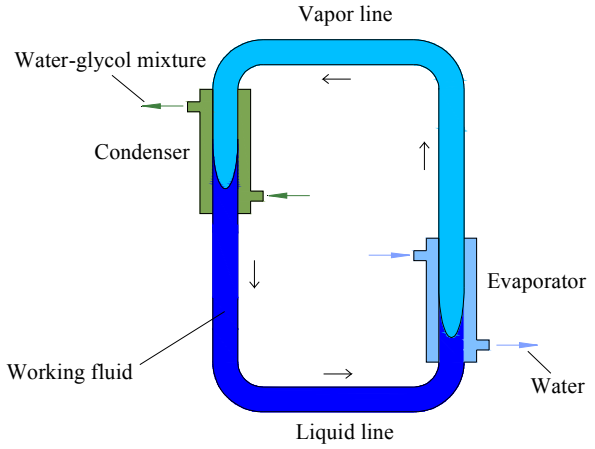

Fig.2. Operating principle of a CLT

The automatic movement of the working fluid is accompanied by heat transfer and can be controlled actively by one or two valves. The two-phase natural circulation flow transfers heat steadily from the evaporator to the condenser when the valves are open. The two-phase natural circulation flow and the heat transfer of CLT cease immediately when the valves are closed. Given that the two-phase natural circulation flow in CLT starts and stops rapidly, CLT can operate intermittently to control heat transfer and the loading temperature. A high start–stop frequency can improve the temperature control precision of CLT significantly.

Experimental facility description

Fig.3 shows the two CLTs designed. The only difference between the two CLTs is the reservoir in the liquid line. R134a was used as the working fluid, and copper was used as the pipe material. The condenser is located above the evaporator, and the vapor line is located between the evaporator outlet and the condenser inlet. The liquid line, which contains a reservoir, connects the condenser outlet to the evaporator inlet. The evaporator and condenser consist of inner tubes with two tube-in-tube helical heat exchangers. A shell inlet and a shell outlet exist in the tube-in-tube helical heat exchanger. Valves 1 and 2 are located on the top of the vapor line and on the bottom of the liquid line, respectively. The geometrical parameters of the CLTs are listed in Table 1.

Fig.3 shows the primary components of the test rig. DC-0515 and DC-3015 were set as the water hot bath and cold bath, respectively. The temperature control range of DC-0515 is from −5 °C to 100 °C and that of DC-3015 is from −30 °C to 100 °C. Their common characteristics of accuracy, maximum flow rate, and total power are 0.1 °C, 10 L/min, and 2.5 kW, respectively. Water was supplied to the evaporator as a heat source, whereas a water–glycol mixture was supplied as the heat sink for the condenser. The temperatures of the supplied water and water–glycol mixture can be varied. The evaporator and condenser heat exchangers were in counter flow. A heat insulation layer was utilized to minimize the cooling loss.

Table 1. Geometrical characteristics of CLT

Component	Inner diameter (mm)	Outer diameter (mm)	Length (m)
Vapor line	10	12	1.3
Liquid line	10	12	1.5
Evaporator	10	12	1.34
Shell of evaporator	23	25	1.34
Condenser	10	12	1.34
Shell of condenser	23	25	1.34
Helical heat exchanger	147	172	1.34
Reservoir (if present)	33	35	0.25

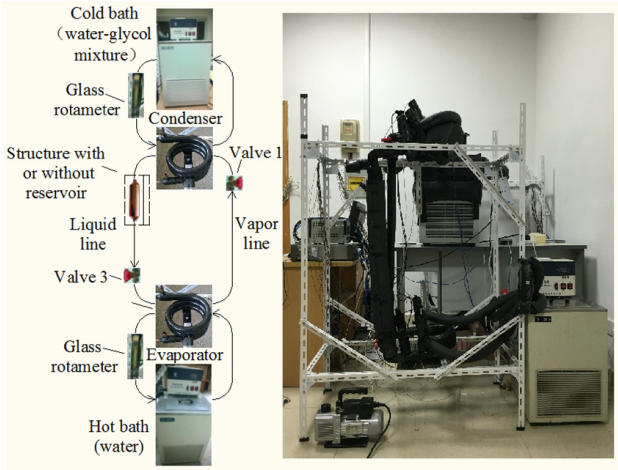

Fig.3. Test rig

Measurements

The measurement points of the CLTs are shown in Fig.4, and a list of experimental testing and monitoring devices is provided in Table 2. The inlet and outlet temperatures of the water–glycol mixture and water were measured with WZP-291 Pt100 platinum resistances. The wall temperatures of the vapor and liquid lines were monitored through numerous T-type thermocouples. The pressures of R134a at the evaporator and condenser inlets were measured with two JT-131 pressure sensors. These measurements were recorded with an Agilent data acquisition instrument every 5 s. The flow rates of the water–glycol mixture and water were measured

with two glass rotameters. An electronic scale was used to measure the mass of R134a filled in CLT.

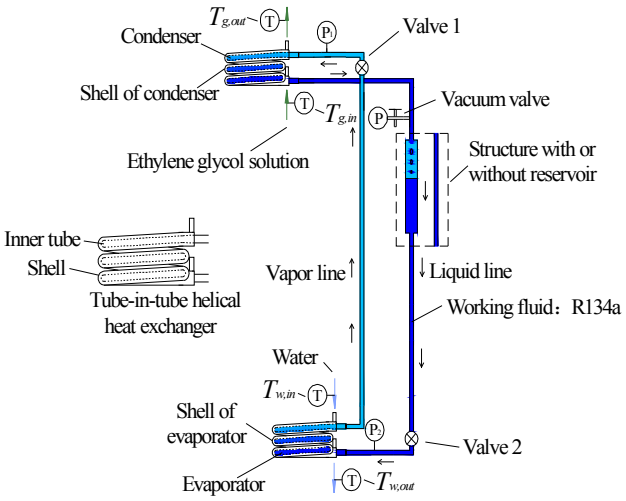

Fig.4. Structure and measurement points of CLTs

Table 2. Experimental testing and monitoring devices

Name	Specification	Accuracy
Pressure sensor	JT-131	0.5%
Platinum resistance	WZP-291 Pt100	±0.1 °C
Thermocouple	T-type	±0.5 °C
Flow meter	Glass rotameter	2.5%
Scale	Electronic	±0.5 g
Data acquisition unit	Agilent 34970	/

EXPERIMENTAL METHODS AND CALCULATION

The water and water–glycol mixture were supplied stably when the valve (or two valves) was closed to simulate the internal environment of a cool-storage refrigerator. When CLT was completely stopped, its heat transfer rate reached zero, and the pressure was constant. The CLT without a reservoir and that with a reservoir were named CLT1 and CLT2, respectively. The time for the heat transfer rate to decrease from 100% to 5% in the stopping process was selected to represent the stopping performance of CLT. The time consumed to reach the maximum heat transfer rate in the start-up process was selected to represent the start-up performance.

Normal test conditions were adopted unless mentioned otherwise and were set as follows. The temperature of the water–glycol mixture supplied from the cold bath was −25 °C, and the temperature of water flowing from the hot bath was 5 °C. The flow rates of the water–glycol mixture and water were set to 80 and 100 L/H, respectively.

Two valves were added to the vapor and liquid lines, so three control modes were available to start and stop the heat transfer process of the CLTs.

(1) Control mode A: The valve located on the vapor line functions as the only switch.

(2) Control mode B: The valve located on the liquid line functions as the only switch.

(3) Control mode C: The two valves function as switches.

The experiment was performed as follows. The R134a fill ratio was verified, and the inlet temperature of the water–glycol mixture was verified from −25 °C to −17 °C. The steady-state heat transfer and start–stop performances of the CLTs with and without a reservoir were tested under different test conditions. Optimal fill ratios were selected for further investigation. The start–stop performance of CLT was then investigated under different experimental conditions.

During the course of the experiment, the transient heat transfer capability of CLT was represented by the heat transfer rate of the evaporator. At any time, the transient heat transfer rate of evaporator can be calculated as follows:

$$Q = \rho V C p (t_{\mathrm{w,in}} - t_{\mathrm{w,out}}), \qquad (1)$$

where V is the transient measured volume flow rate of water and $t_{\mathrm{w,in}}$ and $t_{\mathrm{w,out}}$ are the transient measured inlet and outlet water temperatures of the evaporator, respectively.

RESULTS AND DISCUSSION

Effect of reservoir on steady-state performance

Experiments were performed on CLT1 and CLT2 at different fill ratios of R134a to analyze the effect of the reservoir on the steady-state working performance of CLT. At each fill ratio, the inlet water–glycol mixture temperature, $t_{\mathrm{g,in}}$, varied from −25 °C to −17 °C. The heat transfer rate of stably operating CLT1 at different R134a fill ratios and $t_{\mathrm{g,in}}$ values is shown in Fig.5. The heat transfer rate of CLT1 for each $t_{\mathrm{g,in}}$ value increased initially and then decreased with an increasing fill ratio. This variation trend was evident when fitted by a cubic spline interpolation curve. The maximum heat transfer point of each curve was defined as the optimal operating point. The fill ratios of optimal working points for different heat sink temperatures varied from 34.74% to 38.9%. In the normal test condition, the maximum heat transfer capability was obtained at a fill ratio of approximately 38.9%. Excessive or insufficient R134a restricted the heat

transfer capability of CLT1. Moreover, the fill ratios of optimal operating points varied with $t_{g,in}$. In the practical application of cool-storage refrigerators, the fill ratio of CLT1 cannot be changed, and this defect would cause a deviation from the ideal working condition if the heat sink temperature is varied.

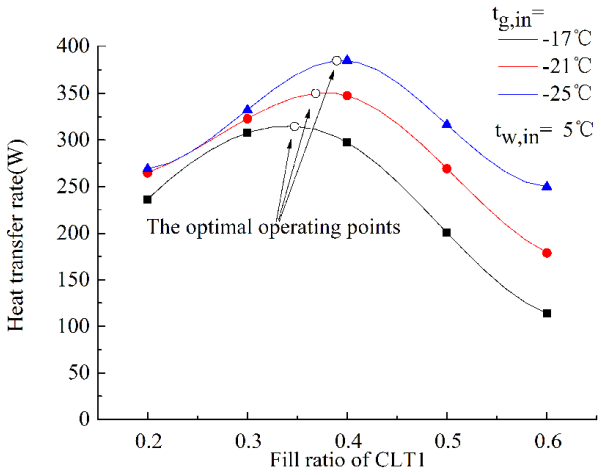

Fig.5. Heat transfer performance of CLT1

Fig.6 shows that using an additional reservoir exerts a remarkable effect on the steady-state heat transfer performance of CLT. The heat transfer rate of CLT2 in normal test conditions was almost unchanged when the R134a fill ratio changed from 32% to 67%. The heat transfer rate of CLT2 decreased when the fill ratio exceeded this suitable range. This suitable range was still valid when $t_{g,in}$ increased. Thus, CLT2 could operate in its optimal working condition even if the heat sink temperature was varied.

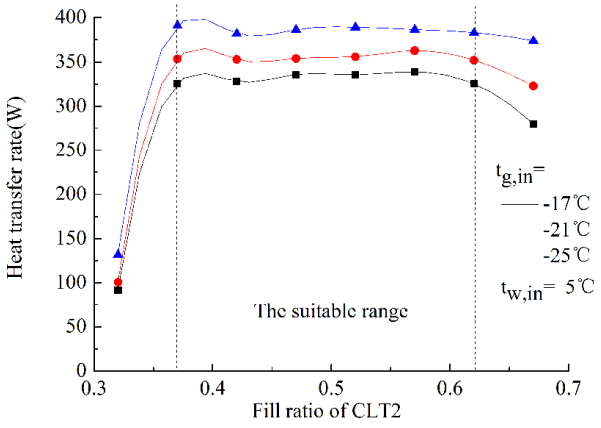

Fig.6. Heat transfer performance of CLT2

Comparison of the heat transfer performance of CLT1 and CLT2 showed that the reservoir can improve the steady-state performance of CLT. The heat transfer stability improvement can be explained as follows. The optimal R134a distribution in the evaporator and condenser changed when the heat sink temperature of CLT without a reservoir varied. Thus, the optimal R134a fill ratio varied with the working environment. CLT1 experienced difficulty reaching and maintaining its optimal working condition. By contrast, in CLT2, the R134a storage function of the reservoir could adjust the R134a distribution in the evaporator and condenser at any time. The CLT with a reservoir could maintain the ideal steady-state heat transfer status because of the wide range of suitable R134a fill ratio.

Effect of reservoir on control stability

The control stability of CLT was tested by starting up and stopping CLT at various R134a fill ratios, control modes, and $t_{g,in}$ values. CLT1 never failed to start or stop during the dozens of tests, and it started and stopped steadily even when the fill ratio deviated from its optimal value and the steady-state heat transfer of CLT1 was degraded seriously. By contrast, several adverse phenomena occurred in the starting process of CLT2. CLT2 could start and stop steadily under different test conditions when the R134a fill ratio varied from 57% to 67%. However, CLT2 could not start up normally under various test conditions when the fill ratio was lower than 57%. The three typical start-up failures are as follows.

1. Fig.7 shows that high-frequency heat transfer and pressure oscillation occurred when CLT2 was initialized in control mode A with a 47% fill ratio. The steady-state heat transfer rate of CLT2 under normal test conditions was approximately 380 W; however, the highest heat transfer rate in this oscillation process was less than 100 W. When CLT2 entered the oscillation state, the oscillation continued for hours, and the circulation flow could not return to normal automatically.

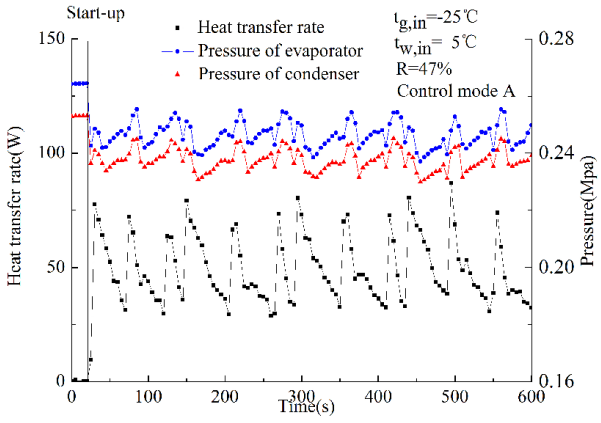

Fig.7. First typical start-up failure of CLT2

2. The second typical start-up failure is shown in Fig.8. CLT2 failed to start up in control mode A again when $t_{g,in}$ was −21 °C and the R134a fill ratio was 52%. No heat transfer and pressure oscillation occurred during this start-up process. However, CLT2 could only maintain a stable low heat transfer. This heat transfer deterioration was unable to recover without artificial interference.

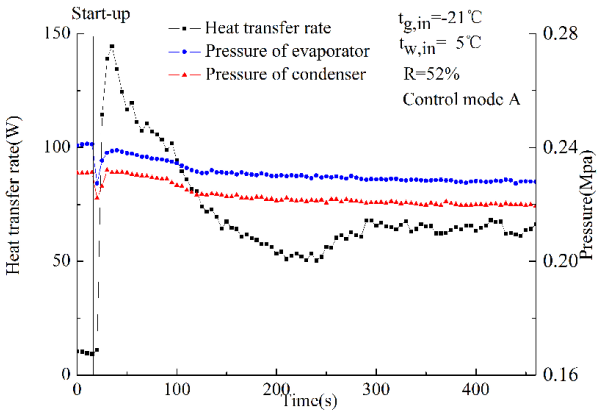

Fig.8. Second typical start-up failure of CLT2

3. Fig.9 shows that the third typical start-up failure appeared in control mode C. The heat transfer rate increased rapidly with pressure when CLT2 was initialized and almost reached stability in approximately 200 s. This period of start-up process was similar to other normal start-up processes of control mode C. However, temporary heat transfer deterioration appeared in about 250 s. This temporary heat transfer deterioration only lasted for 200 s and disappeared after pressure fluctuation within a narrow range. The recovery process was similar to a normal start-up process and did not require artificial interference. CLT2 reached its stable operating state after this temporary heat transfer deterioration in the start-up process.

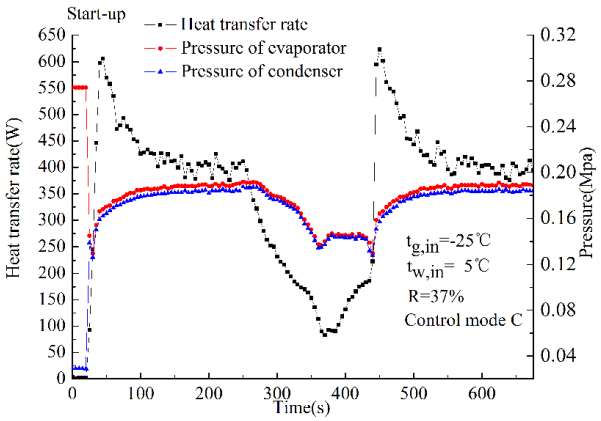

Fig.9. Third typical start-up failure of CLT2

The abovementioned typical cases show the unstable control performance of CLT2. Such unstable phenomena may be caused by a reservoir with a low liquid level height. We recommend that CLT2 be operated at an R134a fill ratio of 57% to 67% to avoid start-up failure. By contrast, CLT1 showed better active control stability than CLT2.

The optimal fill ratio of CLT2 was approximately 62% because of its excellent start–stop performance and good steady-state heat transfer capability. The optimal fill ratio of CLT1 under normal test conditions was determined in our previous study, and the value is 38.9% [26]. The following start–stop performance comparison between CLT1 and CLT2 was based on their optimal fill ratios.

Effect of reservoir on start–stop performance

The three control modes of CLT were well investigated in our previous work. The results showed that the start–stop performance of control mode C is the best, that of control mode A is acceptable, and that of control mode B is not recommended [26]. Thus, in the present study, control modes A and C were tested to compare the start–stop performances of CLT1 and CLT2.

We performed experiments with different $t_{g,in}$ values. CLT1 and CLT2 were tested to analyze the effect of the reservoir on the start–stop performance of control mode A. A comparison of the results is shown in Fig.10. For convenience, heat transfer rate and pressure are denoted by Q and P, respectively. In control mode A, the start-up of CLT1 and CLT2 was quite rapid, and the time consumed to reach the maximum heat transfer rate was approximately 15–20 s. The heat transfer rates of CLT1 and CLT2 were also similar after a stable working status was reached. However, the time consumed for heat transfer stabilization differed.

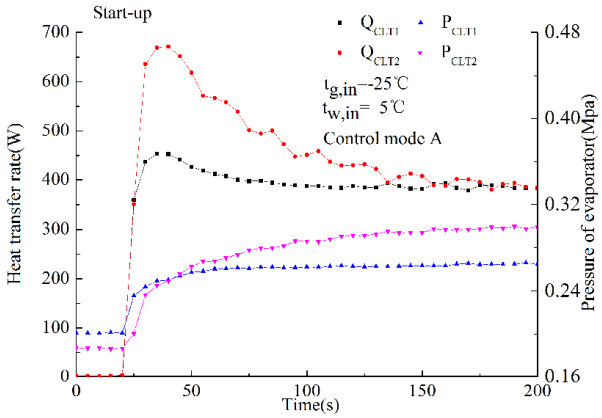

Fig.10. Comparison of start-up processes in control mode A

The heat transfer rate and pressure of CLT1 in the start-up process stabilized in 100 s, whereas

those of CLT2 required twice as much time. Temporary heat transfer enhancements appeared in the early start-up processes, and that of CLT2 was much stronger than that of CLT1. Fig.11 shows the stopping processes in control mode A at normal test conditions. The heat transfer of CLT1 stopped in approximately 100 s and was faster than that of CLT2. The evaporator pressure of CLT1 increased temporarily before it steadily declined and reached stability in 400 s. Fig.10 and Fig.11 show that the stable operating and stopping pressures of CLT1 differed from those of CLT2.

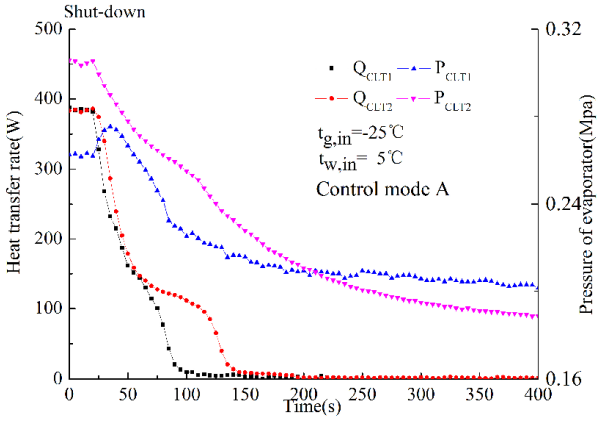

Fig.11. Comparison of stopping processes in control mode A

$t_{g,in}$ was varied from −25 °C to −17 °C to analyze the start–stop performance difference between CLT1 and CLT2 in control mode A. The start-up time stabilized within 15–25 s. However, various differences were observed in control mode A. Table 3 shows that the steady-operating and steady-stopping evaporator pressures and the heat transfer stopping time increased gradually with $t_{g,in}$. Moreover, the operating pressures of CLT1 at various $t_{g,in}$ values were higher than those of CLT2, contrary to the stopping pressures. These phenomena in the start–stop process of control mode A can be explained as follows.

Table 3. Stopping time of CLT1 and CLT2 at various $t_{g,in}$ values in control mode A

$t_{g,in}$ (°C)	Stopping time (s)		Operating pressure (Mpa)		Stopping pressure (Mpa)	
	CLT1	CLT2	CLT1	CLT2	CLT1	CLT2
−25	75	120	0.263	0.302	0.202	0.187
−23	75	125	0.267	0.305	0.211	0.197
−21	80	130	0.270	0.306	0.222	0.207
−19	85	145	0.276	0.308	0.233	0.218
−17	95	155	0.279	0.310	0.245	0.230

The additional reservoir stored much R134a. Thus, R134a needed more time to reach stability in the stopping process.The reservoir also decreased the R134a liquid level. Hence, the degrees of overheating in the evaporator and overcooling in the condenser decreased, and the average temperature of R134a increased with pressure. In the steady-state operating process, more liquid R134a extruded from the evaporator by hot vapor in CLT2, and more liquid R134a was affected by the low temperature of the condenser.

The active control abilities of CLT1 and CLT2 in control mode C were tested under normal test conditions. The results were compared. Fig.12 shows that the heat transfer variations of the CLTs in the start-up process were similar to those in control mode A. Their heat transfer began quickly, and CLT2 required more time than CLT1 to reach stability. The evaporator pressures in control mode C decreased rapidly at first and then increased slowly. The time wasted for CLT2 to reach a stable operating status was approximately 150 s, which is triple the time consumed by CLT1.

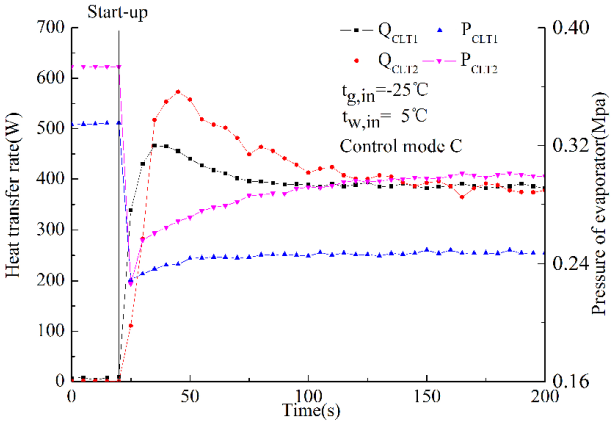

Fig.12. Comparison of start-up processes in control mode C

The stopping processes of CLT1 and CLT2 are shown in Fig.13. The heat transfer and pressure variations are similar. The stopping time of CLT1 and CLT2 is approximately 70–80 s. Their evaporator pressures increased slowly and reached stability in approximately 100 s. The above similarity was retained even when the test conditions were varied. The start–stop performance of control mode C was hardly affected by the reservoir structure unlike that of control mode A primarily because of the unique control method of control mode C. The evaporator in control mode C was isolated from the condenser and reservoir completely when CLT was stopped; thus, the

variations in R134a state in the start-up and stopping processes were unrelated to the reservoir.

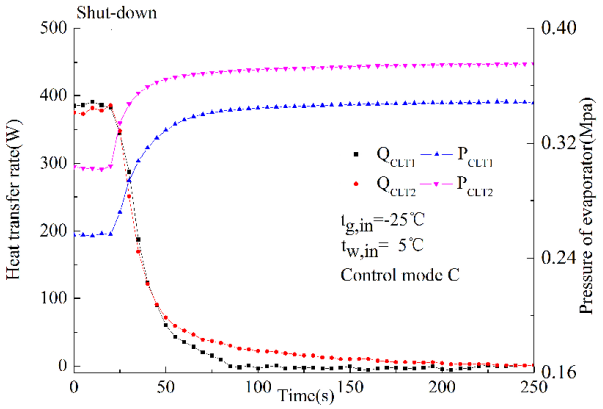

Fig.13. Comparison of stopping processes in control mode C

CONCLUSIONS

We designed and arranged two test rigs to investigate the effect of a reservoir on CLT. Tests were conducted with various R134a fill ratios under normal test conditions to compare the steady-state heat transfer and start–stop performances of the two CLTs. The CLT1 and CLT2 were studied at their optimal R134a fill ratios. The heat sink temperature varied. The following conclusions were obtained.

1. The optimal heat transfer performance of CLT1 was obtained at a fill ratio of 38.9% under normal test conditions. The fill ratios of the optimal working points varied from 38.9% to 34.74% at different $t_{g,in}$ values. CLT2 could operate well at any fill ratios within the range of 32%–67% at each $t_{g,in}$ value. The results showed that a reservoir can remarkably improve the steady-state heat transfer stability of CLT.

2. The CLT without a reservoir displayed a significant advantage in control stability. CLT1 never failed to start or stop even when the fill ratio deviated from its optimal value and the steady-state heat transfer performance was degraded seriously. CLT2 could start steadily under different test conditions when the R134a fill ratio varied in the range of 57%–67%. Several unstable start-ups occurred in the starting process of CLT2 at a fill ratio of less than 57%.

3. The effect of the reservoir on the start–stop performance of CLT revealed clear distinctions among the control modes, which were evident in the stopping process. In control mode A, the additional reservoir increased the stopping time obviously at each $t_{g,in}$ value. Thus, the reservoir could degrade the active control performance of control mode A. By contrast, the start–stop time of CLT1 and CLT2 in control mode C was similar. This result indicates that the active control performance of control mode C was hardly affected by the reservoir structure.

The optimal system design can be selected under different application backgrounds. To obtain good steady-state heat transfer and start–stop performances, the CLT without a reservoir needs to be operated with its optimal R134a fill ratio. The CLT with a reservoir should be operated in control mode C with an R134a fill ratio of 57%–67%.

ACKNOWLEDGEMENT

The study was sponsored by the National Science Foundation of China (NSFC 51476159 and 51206154), Dongguan Innovative Research Team Program (No. 2014607101008), and National Science and Technology Support Program (No. 2015BAD19B02).

NOMENCLATURE

C_p: Specific heat capacity of water (J/(kg·K))
P: Pressure of the evaporator (Mpa)
Q: Heat transfer capability of CLT (W)
R: R134a fill ratio
$t_{g,in}$: Inlet water–glycol mixture temperature of the condenser (°C)
$t_{w,in}$: Inlet water temperature of the evaporator (°C)
$t_{w,out}$: Outlet water temperature of the evaporator (°C)
V : Measured volume flow rate of water (m^3/s)
ρ: Density of water (kg/m^3)

REFERENCES

1 Kim D. S., Ferreira .C A. I., Solar refrigeration options–a state-of-the-art review, International Journal of refrigeration, Elsevier, 31, (2008).
2 El Tom, O. M. M., et al., Performance of a photovoltaic solar refrigerator in tropical climate conditions, Renewable energy, Elsevier, 1 (1991).
3 Long, Rui, et al., Performance analysis of a solar-powered electrochemical refrigerator, Chemical Engineering Journal, Elsevier, 284 (2016).
4 Kattakayam T. A. and Srinivasan K., Lead acid batteries in solar refrigeration systems, Renewable energy, Elsevier, 29 (2004).
5 Siaka Toure and Fassinou W. F., Technical note Cold storage and autonomy in a three compartments photovoltaic solar refrigerator: experimental and thermodynamic study, Renewable energy, Elsevier, 17, (1999).
6 R.E. Foster, D. Bergeron, Photovoltaic Direct Drive Refrigerator with Ice Storage: Preliminary

Monitoring Results, in: ISES 2001 Solar World Congress, 2001.
7 Azzouz K., Leducq D. and Gobin D., Enhancing the performance of household refrigerators with latent heat storage: An experimental investigation, international Journal of Refrigeration, Elsevier, 32, (2009).
8 Subramaniam P, Tulapurkar C, Thiyagarajan R, et al., Phase change materials for domestic refrigerators to improve food quality and prolong compressor off time, International refrigeration and air conditioning conference, Purdue, USA, (2010).
9 MD. Imran Hossen Khan and Hasan M. M. Afroz, Experimental investigation of performance improvement of household refrigerator using phase change material, International journal of air-conditioning and refrigeration, Elsevier, 21, (2013).
10 C. Del Pero, F.M. Butera et al., Feasibility study of a Solar Photovoltaic Adaptable Refrigeration Kit for remote areas in developing countries, 2015 International Conference on. IEEE, 2015.
11 Torriti, J., Price-based demand side management: Assessing the impacts of time-of-use tariffs on residential electricity demand and peak shifting in Northern Italy, Energy, Elsevier, 44, (2012).
12 Barzin R., Chen J. J. Chen, Young B. R., et al, Peak load shifting with energy storage and price-based control system, Energy, Elsevier, 92, (2015).
13 Sekhar, S. Joseph, D. Mohan Lal, and S. Renganarayanan, Improved energy efficiency for CFC domestic refrigerators retrofitted with ozone-friendly HFC134a/HC refrigerant mixture, International journal of thermal sciences, Elsevier, 43, (2004).
14 Jung D, Kim C B, Song K, et al., Testing of propane/isobutane mixture in domestic refrigerators, International journal of refrigeration, Elsevier, 23, (2000).
15 James S. J. and Evans J., The temperature performance of domestic refrigerators, International Journal of Refrigeration, Elsevier, 15, (1992).
16 Amir Faghri, Heat Pipe Science and Technology, Global Digital Press, Washington, 1995.
17 Rahmatollah Khodabandeh, Richard Furberg, Heat transfer, flow regime and instability of a nano- and micro-porous structure evaporator in a two-phase thermosyphon loop, International Journal of Thermal Sciences, Elsevier, 49, (2010).
18 Yu Song, Aurélien Four and Bertrand Baudouy, Nucleate boiling heat transfer in a helium natural circulation loop coupled with a cryocooler, International Journal of Heat and Mass Transfer, Elsevier, 66, (2013).
19 Jiang He, Guiping Lin et al., Effect of non-condensable gas on startup of a loop thermosyphon, International Journal of Thermal Sciences, Elsevier, 72, (2013).
20 A.A. Chehadea, H. Louahlia-Gualous et al., Experimental investigation of thermosyphon loop thermal performance, Energy Conversion and Management, Elsevier, 84, (2014).
21 Ali Chehadea, Hasna Louahlia-Gualous et al., Experimental investigations and modeling of a loop thermosyphon for cooling with zero electrical consumption, Applied Thermal Engineering, Elsevier, 87, (2015).
22 Ji Lia, Feng Linb, Gengwen Niu, An insert-type two-phase closed loop thermosyphon for split-type solar water heaters, Applied Thermal Engineering, Elsevier, 70, (2014).
23 Penglei Zhang, Baolong Wang, Wenxing Shi, Xianting Li, Experimental investigation on two-phase thermosyphon loop with partially liquid-filled downcomer, Applied Energy, Elsevier, 160, (2015).
24 Zhen Tong, Tao Ding, Zhen Li, Xiao-Hua Liu, An experimental investigation of an R744 two-phase thermosyphon loop used to cool a data center, Applied Thermal Engineering, Elsevier, 90, (2015).
25 Alessandro Franco and Sauro Filippeschi, Closed Loop Two Phase Thermosyphon of Small Dimensions: a Review of the Experimental Results, Microgravity Sci. Technol., Elsevier, 24 (2012).
26 Jingyu Cao, Jing Li and Gang Pei, Performance Evaluation of Controllable Loop thermosyphons, Applied Thermal Engineering, Elsevier, 100 (2016).